RSC Chemical Biology

ROYAL SOCIETY OF CHEMISTRY

PAPER

View Article Online
View Journal | View Issue

Cite this: *RSC Chem. Biol.*, 2025, 6, 281

A one-step route for the conversion of Cd waste into CdS quantum dots by *Acidithiobacillus* sp. *via* unique biosynthesis pathways†

Xiao-Ju Li, ‡*[a] Tian-Qi Wang,‡[a] Lu Qi,‡[b] Feng-Wei Li,[a] Yong-Zhen Xia,[a] Bin-Jin,[c] Cheng-Jia Zhang,[a] Lin-Xu Chen*[a] and Jian-Qun Lin*[a]

Microorganisms serve as biological factories for the synthesis of nanomaterials such as CdS quantum dots. Based on the uniqueness of *Acidithiobacillus* sp., a one-step route was explored to directly convert cadmium waste into CdS QDs using these bacteria. First, an exhaustive study was conducted to reveal the specific pathways involved in the biosynthesis of CdS QDs. The widely known homologous enzyme, cysteine desulfhydrase, which catalyzes the synthesis of CdS QDs from a cysteine substrate, is also present in *Acidithiobacillus* sp. and is referred to as the OSH enzyme. The structure of the OSH enzyme was determined through X-ray crystallography. Moreover, we identified two new pathways. One involved the SQR enzyme in *Acidithiobacillus* sp., which catalyzed the formation of sulfur globules and subsequently catalyzed further reactions with GSH to release H_2S; subsequently, a CdS QD biosynthesis pathway was successfully constructed. The other pathway involved extracellular polyphosphate, a bacterial metabolic product, which with the addition of GSH and Cd^{2+}, resulted in the formation of water-soluble fluorescent CdS QDs in the supernatant. Based on the above-described mechanism, after the bioleaching of Cd^{2+} from cadmium waste by *Acidithiobacillus* sp., CdS QDs were directly obtained from the bacterial culture supernatants. This work provides important insights into cleaner production and cadmium bioremediation with potential industrial applications.

Received 19th August 2024,
Accepted 19th December 2024

DOI: 10.1039/d4cb00195h

rsc.li/rsc-chembio

1. Introduction

Semiconductor nanoparticles, known as quantum dots (QDs), have attracted significant interest over the last three decades because of their unique quantum confinement properties. Optical properties, such as tunable light emission, are observed in cadmium sulfide (CdS) QDs, making them applicable in fields such as light-emitting devices, sensory materials, and bioassays.[1,2] Several chemical methods have been utilized for synthesizing CdS QDs. However, these methods typically require toxic reagents, hazardous organic solvents, and extreme reaction conditions, leading to substantial organic and inorganic pollutant emissions into air, water, and soil.[3–6] Furthermore, achieving water-soluble and biocompatible QDs through chemical synthesis remains a challenge, necessitating time-consuming post-synthetic processing or specialized strategies,[1,7–11] such as protein-QD hybrids involving bovine serum albumin, lysozyme, trypsin, hemoglobin, transferrin, or poly(histidine) fusion proteins.

Current research focuses on the biosynthesis of sulfide QDs using biological systems, effectively addressing the aforementioned limitations. Various biological resources, including bacteria, yeasts, fungi, algae, viruses, plants, and plant extracts, have been harnessed for the economical and environmentally friendly bioproduction of sulfide QDs.[12] Unlike chemical synthesis methods, biosynthesis requires less energy and avoids the use of toxic reductants and surfactants. Microorganisms can synthesize sulfide QDs in nontoxic solvents, primarily water, under mild conditions. This biosynthetic approach utilizes biological processes to guide reaction steps and material structures, yielding sulfide QDs with comparable electronic, photochemical, and optical properties to those synthesized chemically. Bacteria and yeast are particularly notable among the organisms used for sulfide QD biosynthesis, with bacteria standing out due to their rapid growth and ease of cultivation

[a] State Key Laboratory of Microbial Technology, Shandong University, Qingdao 266237, China. E-mail: lixiaoju@sdu.edu.cn, linxuchen@sdu.edu.cn, jianqunlin@sdu.edu.cn
[b] Science Center for Material Creation and Energy Conversion, Institute of Frontier and Interdisciplinary Science, Shandong University, Qingdao 266237, China
[c] Institute of Molecular Sciences and Engineering, Institute of Frontier and Interdisciplinary Science, Shandong University, Qingdao 266237, China

† Electronic supplementary information (ESI) available: PDB 9IQH contains the supplementary crystallographic data for this paper. See DOI: https://doi.org/10.1039/d4cb00195h

‡ These authors contributed equally: Xiao-Ju Li, Tian-Qi Wang, Lu Qi.

compared to other microbial cells.[13–15] The biosynthesis of nanocrystals by bacteria usually involves precise tailoring of their size and crystallinity because of their single-compartment properties. These nanocrystals are regarded as effective green nanofactories for the production of nanoparticles.

Recently, engineered *Escherichia coli* strains were successfully constructed to precipitate CdS QDs intracellularly by overexpressing the foreign genes encoding cysteine desulfhydrase or a CdS-binding peptide.[16–19] In addition, many other bacteria such as *Stenotrophomonas maltophilia*, *Bacillus cereus*, lithobiotic Antarctic strains, and deep-sea salt-tolerant strains have also been reported to biosynthesize CdS QDs.[20–26] In various microbial culture systems, the addition of cysteine is crucial for the biosynthesis of CdS QDs, as it stimulates the production of hydrogen sulfide (H_2S), facilitating the formation of QDs such as cadmium sulfide. Furthermore, electrospray mass spectrometry has identified cysteine desulfhydrase, an enzyme homolog present in these microorganisms,[20] which catalyzes various elimination reactions, including the breakdown of cysteine into H_2S, pyruvate, and NH_3. Through methods involving heterologous expression, protein purification, and *in vitro* functional assays, researchers have demonstrated that recombinant cystathionine γ-lyase, a homologous enzyme to cysteine desulfhydrase, can catalyze the production of CdS QDs. This enzyme facilitates the mineralization of CdS from an aqueous cadmium acetate solution by generating reactive H_2S from cysteine. In some microorganisms, this type of enzyme has the ability to efficiently synthesize CdS QDs.[27,28] Additionally, extensive structural analyses have been performed on cystathionine γ-lyase.[29,30]

Acidithiobacillus sp., a distinct class of chemoautotrophic bacteria, thrives in environments devoid of organics with a pH typically less than 3. They utilize inorganic sulfur as an energy source, oxidizing it to various sulfates to sustain themselves. Their metabolic products including inorganic and organic acids aid in the bioleaching of metals such as copper, nickel, zinc, chromium, cadmium, and lead from minerals or waste materials. Owing to their unique metabolic abilities, *Acidithiobacillus* sp. exhibits remarkable tolerance to heavy metals, notably cadmium, even at concentrations as high as 200 mM.[31–33] For the past three decades, *Acidithiobacillus* sp. has been extensively utilized in biohydrometallurgy for mineral bioleaching. Although cadmium is one of the most toxic heavy metals and poses a serious threat to human health, it continues to be used in certain industries because of its distinctive properties in applications such as electroplating and batteries, resulting in unavoidable cadmium waste. These findings underscore the urgent need for strategies to dispose cadmium pollution and efficiently recover cadmium waste safely. Recent research has focused on the use of *Acidithiobacillus* sp. in the remediation of heavy metal pollution, where they play a significant role.[34–37] Studies have demonstrated their effectiveness in bioleaching cadmium from Ni–Cd battery electrodes into a solution during *Acidithiobacillus* sp. cultivation.[34] However, the subsequent treatment of these bleached cadmium solutions remains a major challenge. Current methods primarily involve chemical approaches such as membrane separation or chemical precipitation.[38,39] However, there is a notable gap in research on biological methods for further treating bioleached cadmium, especially in the conversion of heavy metal waste into valuable resources, an area in urgent need of development.

Like many reported microorganisms for CdS QD biosynthesis,[16–26] the ability of *Acidithiobacillus* sp. to biosynthesize CdS QDs with the addition of cysteine and Cd^{2+} sources has also been confirmed.[40] However, the detailed mechanisms of CdS QD biosynthesis in *Acidithiobacillus* sp. have not been revealed. The direct biosynthesis of CdS QDs from real industrial cadmium waste by using microorganisms has not been explored, but it has strong practical significance for energy conservation and broad application prospects for sustainable development.

Because *Acidithiobacillus* sp. are chemoautotrophic bacteria that use inorganic sulfur as energy, they have unique and complex sulfur metabolic mechanisms, which were systematically studied in our previous work.[32,41] Various enzymes related to inorganic sulfur metabolism and their functions, including elemental sulfur (S), hydrogen sulfide (H_2S), thiosulfate ($S_2O_3^{2-}$), and tetrasulfate ($S_4O_6^{2-}$), have been discovered and validated; these enzymes are important sulfur metabolites that undergo transformation between substances through corresponding enzymes, ultimately achieving complete oxidation from elemental sulfur to sulfate. Our analysis revealed that the homologous enzyme cysteine desulfhydrase, which is a key enzyme for CdS QD biosynthesis, is also present in *Acidithiobacillus* sp. and is known as the O-succinylhomoserine sulfhydrylase (OSH) enzyme. Furthermore, our study revealed that in addition to the ability of the OSH enzyme to induce the production of H_2S, other enzymes related to H_2S production, such as the sulfide-quinone reductase (SQR) enzyme, still exist.[42,43] In addition, many substances are produced during the culture process, during which inorganic sulfur is used as energy for *Acidithiobacillus* sp. Therefore, in this work, the relationships between CdS QD biosynthesis and various enzymes in *Acidithiobacillus* sp. were investigated in detail, and how these associated products promote CdS QD biosynthesis during inorganic sulfur transformation in *Acidithiobacillus* sp. was also revealed.

Furthermore, based on our investigation of the mechanisms underlying the biosynthesis of CdS QDs by *Acidithiobacillus* sp., we exploited a valuable strategy for solid cadmium waste recycling by *Acidithiobacillus* sp. In this strategy, after the bioleaching of Cd from solid cadmium electroplating waste to a solution by *Acidithiobacillus* sp., we further used this bioleaching process as a Cd^{2+} source, together with *Acidithiobacillus* sp. cultivation, to successfully realize the direct biosynthesis of CdS QDs. The direct use of cadmium waste as a feedstock for the biosynthesis of CdS QDs is a promising approach for producing this waste. Two main industrially used microorganisms, *Acidithiobacillus* sp. containing *Acidithiobacillus ferrooxidans* (*A. ferrooxidans*) ATCC23270 and *Acidithiobacillus caldus* (*A. caldus*) MTH-04, were used as our research objects in this work. This work may facilitate a better understanding of the biosynthetic

mechanism of nanomaterials and contribute to its application in environmental remediation.

2. Results and discussion

2.1. Biosynthesis of CdS quantum dots by the OSH enzyme

Cysteine desulfhydrase, a crucial enzyme in organic sulfur metabolism across organisms, catalyzes the production of H_2S during cysteine reactions. The homologous enzyme cystathionine γ-lyase has been shown to utilize cysteine as a substrate, generating H_2S, which catalyzes the synthesis of CdS QDs from an aqueous cadmium acetate solution.[29] BLAST searches of the NCBI database revealed that the homologous enzyme also exists in *Acidithiobacillus* sp. and is named the *O*-succinylhomoserine sulfhydrylase (OSH) enzyme. In this study, the OSH enzymes from *A. ferrooxidans* (NCBI reference no. WP_012536942.1) and *A. caldus* (NCBI reference no. WP_004873154.1) were heterologously overexpressed and purified from *Escherichia coli*. Expression and purification using immobilized metal affinity chromatography resulted in a single 42 kDa protein (Fig. S1, ESI†). To assess the function of the OSH enzyme, a solution containing cysteine (4 mM) and cadmium acetate (0.5 mM) was prepared in aqueous Tris buffer (pH 8.0) with the OSH enzyme (1 mg mL^{-1}). The reaction progress was monitored over time at ambient temperature and pressure *via* UV-visible and fluorescence spectroscopy.

Fig. 1 depicts the outcomes of the purified OSH enzyme from *A. caldus*, demonstrating its ability to directly control the synthesis of CdS QDs from aqueous solutions using cysteine and cadmium acetate as reactants. Both the absorption (Fig. 1b) and fluorescence (Fig. 1c) peaks exhibited systematic shifts with longer growth times in culture. The redshift observed in the absorbance and fluorescence maxima suggested an increase in the average size of the CdS nanoparticles over the course of the incubation period. A similar result was also observed for the ability of the purified OSH enzyme from *A. ferrooxidans* to catalyze CdS synthesis (Fig. S2, ESI†). However, when glutathione (GSH) and cadmium acetate are used as reactants for CdS QD synthesis by the OSH enzyme, the generation of CdS nanoparticles requires a relatively long time, suggesting that GSH is not an ideal reactant for the OSH enzyme (Fig. S3, ESI†), which is very different from the reported cystathionine γ-lyase.[29]

In this research, the atomic-level structure of the OSH enzyme from *A. ferrooxidans* was determined using X-ray crystallography, as shown in Fig. 1d and e, which show the crystalline photograph and structure, respectively. Molecular replacement with *O*-succinylhomoserine sulfhydrylase (PDB: 3NDN), a similar enzyme from *Mycobacterium tuberculosis*, facilitated structure determination. The detailed data collection, phasing, and refinement statistics can be found in Table S1 (ESI†). OSH is structured as a dimer in the asymmetric unit, with both monomers closely resembling each other (Fig. 1e). Each OSH monomer contains a pyridoxal phosphate (PLP) molecule (Fig. S4, ESI†), a recognized prosthetic group in this enzyme class. The structure of OSH obtained in this work is very different from that of other previously characterized cystathionine γ-lyases, which consist entirely of tetramers in one asymmetric unit with two symmetry-related dimers.[30] This may explain why the efficiency of the biosynthesis of CdS QDs by the OSH enzyme from *Acidithiobacillus* sp. is much lower than that of the previously reported cystathionine γ-lyase.[29]

2.2. Biosynthesis of CdS quantum dots by the SQR enzyme

There are very unique and complex sulfur metabolic mechanisms in *Acidithiobacillus* sp., as they are completely chemoautotrophic bacteria that use inorganic sulfur as energy.[32,41] In addition to the OSH enzyme in *Acidithiobacillus* sp., which catalyzes CdS QD biosynthesis, we found that other enzymes in *Acidithiobacillus* sp., such as sulfide-quinone reductase (SQR), can also promote H_2S production.[42,43] Our earlier study elucidated a pathway in heterotrophic bacteria that utilizes the SQR enzyme to convert toxic H_2S into relatively benign sulfur globules.[42] The detailed mechanism is outlined in Fig. S5 (ESI†). Through this mechanism, the intermediate product produced during the SQR enzyme oxidation of H_2S further reacts with GSH and releases H_2S. Consequently, how to use this pathway properly for CdS QDs was explored in subsequent work.

The SQR enzyme is also critical in the sulfur metabolism of *A. caldus*. Two sqr genes, *orf* 1436 (SQR1) and *orf* 2678 (SQR2), were identified in the genome *of A. caldus* MTH-04. This work explored the ability of the SQR enzyme to catalyze CdS biosynthesis. First, the two SQR enzymes in *A. caldus* were both heterologously overexpressed in *Escherichia coli*. SQR1 and SQR2 are located on the cytoplasmic membrane, and their active sites are both in the cytoplasm, as the final products of sulfur globules aggregate in the intracellular cells of the recombinant *E. coli* (see Fig. S6 and S7 (ESI†) for our detailed transmission electron microscopic (TEM) observations).

The SQR2 enzyme was subsequently purified for further analyses, and compared with SQR1, SQR2 had greater enzyme activity. The recombinant *E. coli* membrane overexpressing SQR2 was harvested as a purified enzyme, which was then resuspended in Tris–HCl buffer [50 mM, 50 μM diethylenetriaminepentaacetic acid, pH = 8.0]. NaHS was added to this solution as an H_2S source, and after incubation for approximately 3 h, H_2S can be completely converted into sulfur globules by the SQR2 enzyme. Fig. 2b and c show the converted sulfur globules in solution. Fig. 2b shows the precipitated sulfur globules, which are approximately 200–500 nm in diameter. Elemental analysis of this region using X-ray energy-dispersive spectroscopy (EDS) (Fig. 2c) revealed a strong S signal. In the next step, cadmium acetate and GSH were added to this solution system, and then the reactant mixture was placed in a shaker at 30 °C and 200 rpm. After different incubation times, the synthesis of CdS QDs was analyzed. Fig. 2d shows the photographs of photoluminescence under UV light at various time intervals. The absorption (Fig. 2e) and fluorescence (Fig. 2f) peaks both shifted systematically with the increase in growth time in the culture. Additional evidence to support the biosynthesis of CdS QDs from this solution was obtained from the TEM images of the resulting CdS QDs.

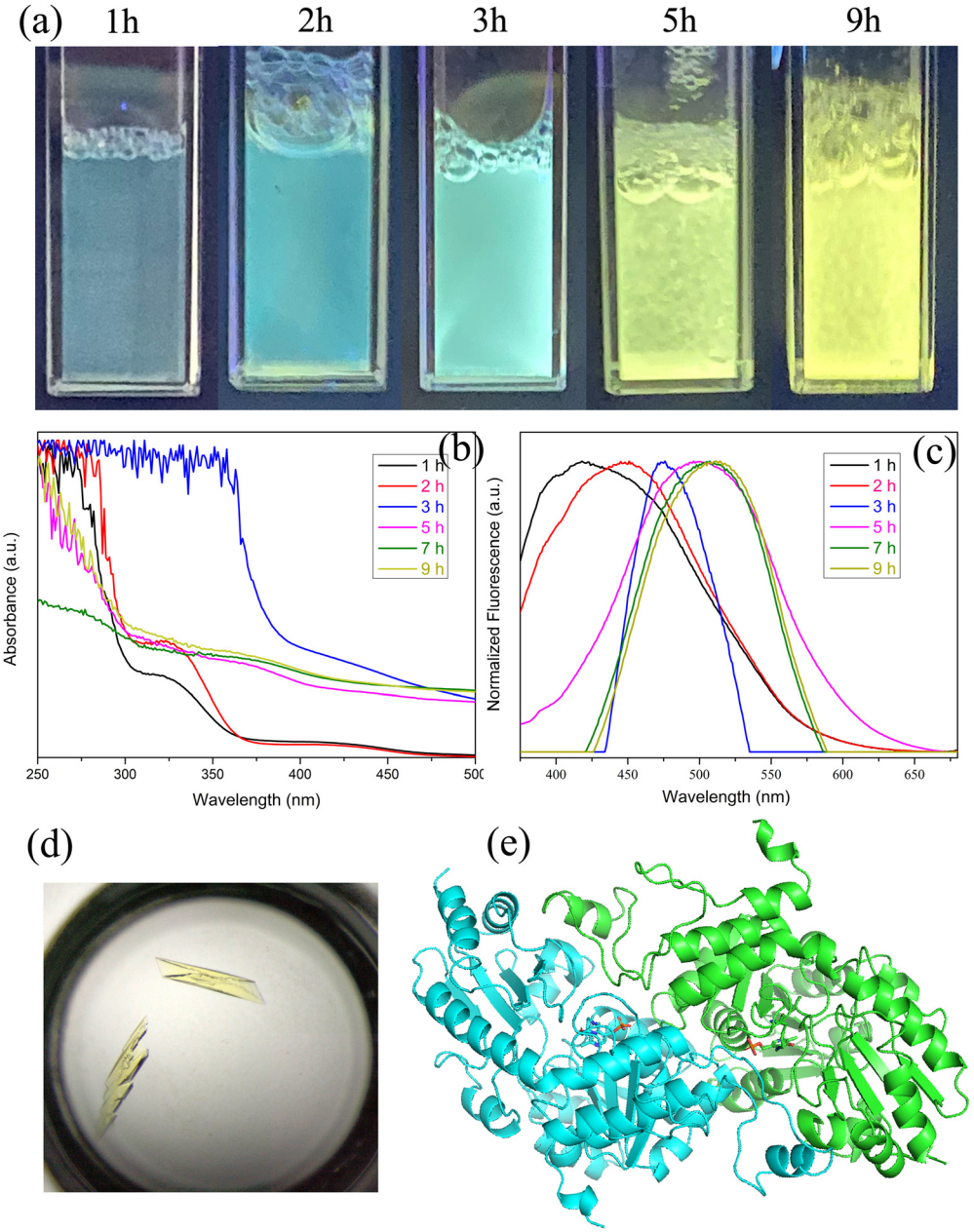

Fig. 1 Optical properties of CdS *versus* synthesis time by the OSH enzyme. (a) Photographs of photoluminescence under UV light at different time intervals. (b) Absorbance spectra of OSH (1 mg mL^{-1}) incubated with 5 mM cysteine and 0.5 mM cadmium acetate for various time intervals. (c) Corresponding fluorescence spectra at selected time intervals using an excitation wavelength of 350 nm. (d) and (e) Crystalline photograph and structure of the OSH enzyme.

Nanoparticles were harvested from the solution after 18 h of growth (with an absorbance maximum of 375 nm) and analyzed by TEM. Fig. 2g shows the existence of discrete but irregularly shaped nanoparticles approximately 5 nm in diameter, and the corresponding selected-area electron diffraction pattern (Fig. 2f) revealed that these nanoparticles were CdS nanocrystals with cubic structures. Fig. 2i shows the X-ray powder diffraction (XRD) pattern of the precipitated CdS nanocrystals after a long reaction time. Two border diffraction peaks centered at approximately 25.48 and 43.73 cm^{-1}, corresponding to the (111) and (220) planes, respectively, also further indicated that cubic CdS is biosynthesized *via* this pathway. Based on the SQR enzyme revealed in our previous work,[42,43] the pathway for CdS QD biosynthesis can be described as follows: the SQR2 enzyme-catalyzed H_2S is converted into sulfur globules, the sulfur globules react with GSH, and then, GSH is oxidized, with H_2S released. The released H_2S reacts with cadmium acetate and simultaneously coordinates with GSH as a capping agent; finally, the CdS QDs are synthesized successfully.

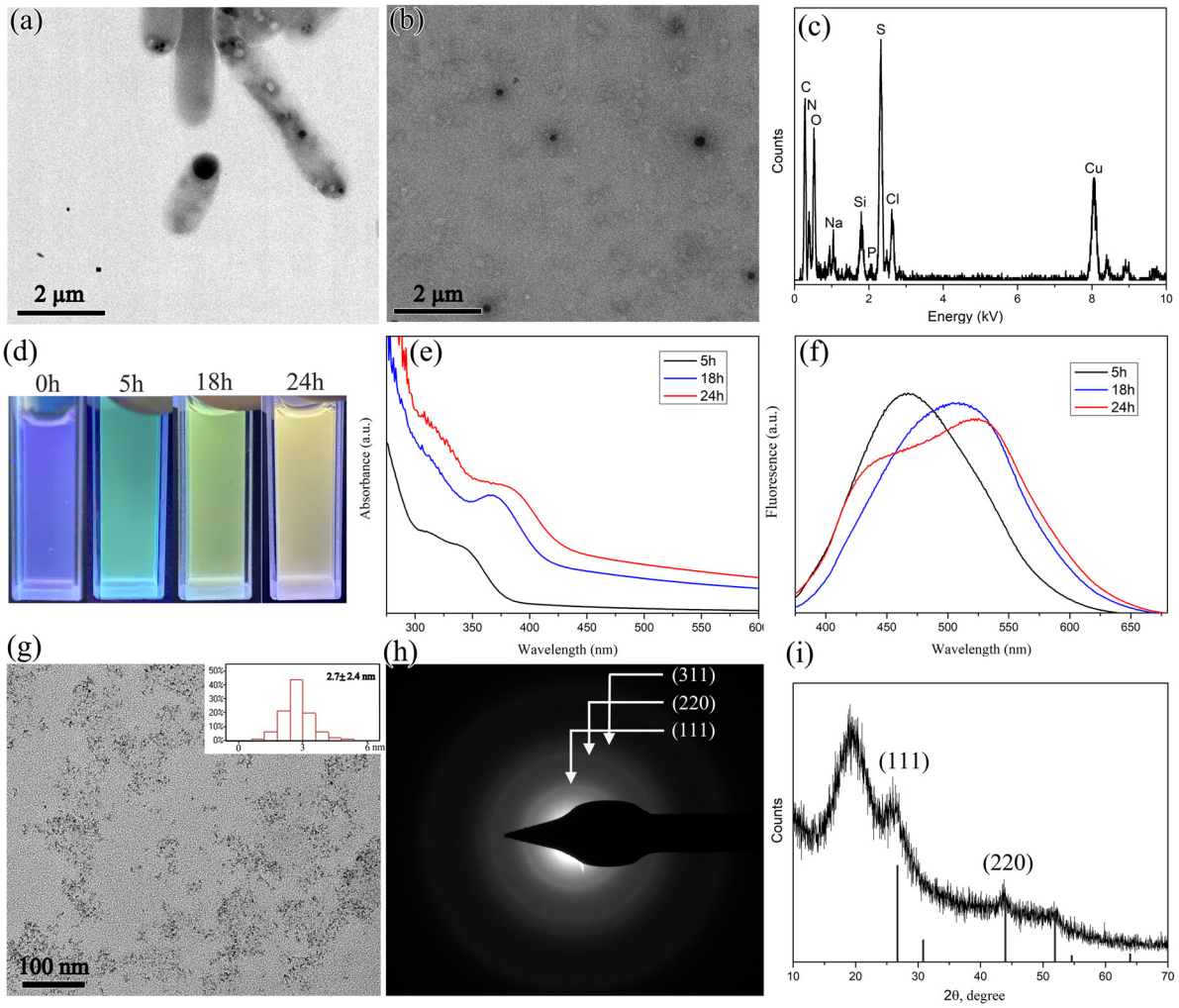

Fig. 2 (a) Transmission electron microscopic (TEM) image of the accumulation of sulfur globules in *Escherichia coli* caused by heterologous overexpression of the SQR2 enzyme. (b) TEM image and (c) energy-dispersive X-ray spectrometry (EDS) of sulfur globules in solution, catalyzed by the collected membrane of recombinant *E. coli* overexpressing SQR2. Further addition of cadmium acetate and GSH to this solution results in CdS QD synthesis. (d) Photographs of photoluminescence under UV light at various time intervals. (e) Absorbance spectra and (f) corresponding fluorescence spectra at selected time intervals at an excitation wavelength of 350 nm. (g) TEM image and corresponding (h) electron diffraction pattern of CdS QDs obtained after 18 h of growth. (i) X-ray powder diffraction (XRD) pattern of the precipitated CdS nanocrystals after a long reaction time.

2.3. Biosynthesis of CdS quantum dots by bacterial culture

During the oxidation of elemental sulfur to sulfate in *Acidithiobacillus* sp., various inorganic sulfur metabolites including elemental sulfur (S), hydrogen sulfide (H_2S), thiosulfate ($S_2O_3^{2-}$), and tetrasulfate ($S_4O_6^{2-}$) undergo transformation between substances through corresponding enzymes.[32,41] Consequently, many substances must be produced during this transformation. Fig. 3(a)–(d) show our new findings on the substances produced in the culture of *A. caldus.* A very unique phenomenon was detected in the *A. caldus* strain when the sulfur dioxygenase gene was knocked out. A number of round spheres are present outside the bacterial cell; these spheres are amorphous and have sizes between 300 and 400 nm. TEM compositional analysis (Fig. 3d) confirmed that these compounds are polyphosphate-like substances. The substances are enriched with phosphate, which may be in the form of polyphosphates. We are the first to observe these extracellular polyphosphates in *Acidithiobacillus* sp. They differ significantly from the well-known intracellular phosphate spheres (Fig. S9, ESI†), as the extracellular polyphosphate spheres are often encapsulated by various substances and recognized as sulfur-enriched substances (Fig. S8, ESI†). This highlights the crucial role of polyphosphates in the metabolism and transformation of inorganic sulfur.

Based on the above-mentioned findings, an alternative pathway for synthesizing CdS QDs from *Acidithiobacillus* sp. was proposed and studied. Polyphosphates, which have been used as effective CdS capping agents,[44,45] were also found to facilitate the release of H_2S from cellular thiols, thereby promoting the synthesis of CdS QDs.[46,47] There must be many polyphosphates in bacterial culture media that are distributed in extracellular cells. This system represents an ideal solution for

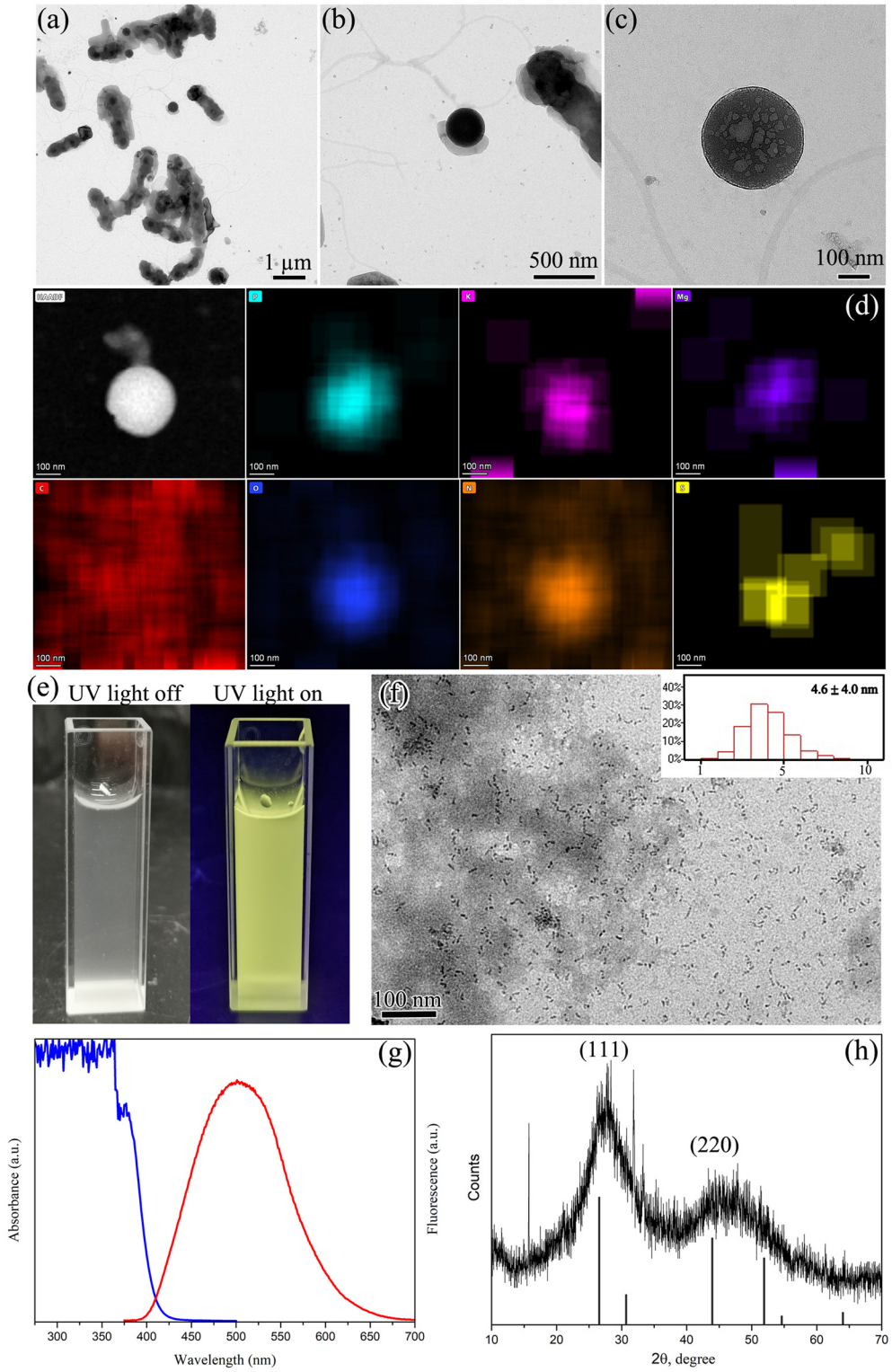

Fig. 3 (a)–(c) TEM images of extracellular polyphosphates distributed in *A. caldus* culture. (d) Elemental maps of one extracellular polyphosphate, indicating that the sphere contains a large number of P, O, N, and K. With respect to extracellular polyphosphates, another pathway for CdS QD biosynthesis is found: (e) photograph of the *A. caldus* culture supernatant under illumination with white light (left) and UV (365 nm) light (right). Yellow fluorescence in the supernatant was clearly observed, implying that the CdS QDs were synthesized successfully. (f) TEM image of the synthesized CdS QDs. (g) Absorbance and corresponding fluorescence spectra of the supernatant at an excitation wavelength of 350 nm and (h) XRD pattern of the synthesized CdS QDs.

CdS QD synthesis. Its major advantage lies in the direct distribution of produced QDs into the extracellular supernatant, eliminating the need for complex purification steps such as cell fragmentation and separation. This simplification significantly reduces the challenges associated with separating biosynthetic QDs. We used sulfur as an energy source to culture *A. caldus*. After the bacteria were cultured to the logarithmic growth phase, they were centrifuged to remove the bacteria, and the resulting supernatant was collected as the solution system. In the next step, cadmium acetate and GSH were added to this solution system, and then the reactant mixture was placed in a shaker at 40 °C and 150 rpm. After 3 days, yellow fluorescence was clearly observed in the solution under UV light (Fig. 3e), and its absorption and fluorescence data are shown in Fig. 3g. The synthesis of CdS QDs was directly observed by TEM (Fig. 3f), and the grown CdS QDs were also obtained and characterized by XRD (Fig. 3h).

The discovery of an extracellular polyphosphate path for CdS QD biosynthesis in *Acidithiobacillus* sp. originated from Venegas *et al.*[46] In their work, without any organisms, inorganic phosphate (Pi) and cellular phosphorylated intermediates such as adenosine monophosphate could trigger CdS QD synthesis. Hence, in our work, we believe that in the absence of bacterial cells, extracellular polyphosphates combined with Cd^{2+} and GSH are sufficient to produce CdS QDs. Its mechanism behind this process must be similar to Venegas' reported job.

Notably, the use of GSH resulted in the ideal result of CdS QD biosynthesis in this solution system; however, when cysteine was used, no CdS QDs clearly distributed in the supernatant could be observed (Fig. S10, ESI†). In addition to sulfur, other energy sources used to culture *A. caldus*, such as $K_2S_4O_6$, can also produce similar results when GSH is added (Fig. S11, ESI†).

Notably, there was obvious spontaneous blue-green fluorescence in the microorganism culture supernatants in our study of the supernatant (Fig. S12–S15, ESI†), which could be a false interference for determining the initial formation of CdS QDs. Strong yellow or orange fluorescence appeared only after the growth of CdS QDs, confirming the successful biosynthesis of the CdS QDs. Spontaneous blue-green fluorescence is observed not only in *Acidithiobacillus* sp. but also in *Escherichia coli*, *Bacillus subtilis*, *etc. Acidithiobacillus* sp. is a unique type of microorganism that survives in acidic environments and produces acid during cultivation. After the *Acidithiobacillus* sp. was cultured to the logarithmic growth phase, the pH of the culture was approximately 0.8, and no spontaneous fluorescence clearly appeared at this low pH. However, once the pH of the culture was adjusted above 4, spontaneous fluorescence clearly appeared (Fig. S13, ESI†). Fig. S14 (ESI†) shows that the inherent fluorescence did not originate from the initial media. The spontaneous fluorescent compounds observed in the culture are presumed to be organic small molecules with molecular weights typically in the hundreds (Fig. S15, ESI†).

2.4. Recycling of cadmium electroplating waste

Our above exhaustive research on the special pathways for CdS QD biosynthesis in *Acidithiobacillus* sp. confirmed that these bacteria have great potential in industrial applications for cadmium waste recycling. Owing to their distinct metabolic processes, the metabolic byproducts of *Acidithiobacillus* sp., including both inorganic and organic acids, play crucial roles in the bioleaching of metals from minerals or wastes and have been extensively studied and applied in industries.[31–37] However, addressing the treatment of bioleaching cadmium solutions remains a great challenge. Naturally, exploring how to utilize *Acidithiobacillus* sp. further to continue treating cadmium ions post-bioleaching, directly converting them into CdS QDs resources, presents a highly promising area of research to enhance waste management practices.

We need to clarify that *A. ferrooxidans* also has SQR enzyme and extracellular polyphosphates. (1) According to the NCBI database, the SQR enzyme also exists in *A. ferrooxidans*. The SQR enzyme is widely present in microorganisms, especially in sulfur autotrophic microorganisms, and acts as an indispensable enzyme. (2) Polyphosphates widely exist in *Acidithiobacillus* sp., including *A. ferrooxidans*, *A. caldus* and *A. thiooxidans.* However, in early studies, polyphosphates were found only in the cells of these bacteria. Our study provides evidence that there are also many polyphosphates distributed extracellularly. (3) The growth temperature of *A. ferrooxidans* (30 °C) is lower than that of *A. caldus* (40 °C); therefore, not only the bacterial growth rate but also the enzyme activity is lower in *A. ferrooxidans*. Considering practical applications, in this study, we focused primarily on *A. caldus*. In subsequent experiments, the wild-type strain of *A. caldus* was used for cadmium waste management.

After approximately 7 days of cultivation with sulfur as the energy source, the culture pH of *A. caldus* was approximately 0.8. The cadmium electroplating waste (Fig. S16 and S17, ESI†) was subsequently introduced into the bacterial culture for bioleaching. Fig. 4a shows the correlation between the quantity of cadmium electroplating waste added and the concentration of cadmium ions bioleached into the bacterial supernatant. The pH of these bioleaching solutions was adjusted from acidic to neutral *via* the addition of KOH, followed by the addition of GSH. After approximately 3 days of reaction, CdS QDs were obtained from the bacterial mixture, as depicted in Fig. 4b, which shows the solution under white light (left) and UV (365 nm) light (right); yellow fluorescence was clearly observed. Photoluminescence persisted in the culture supernatants even after the cells were removed by centrifugation, indicating that most water-soluble fluorescent particles were produced extracellularly. Although some CdS QDs that precipitated around the extracellular polymeric substances (EPS) surrounding the bacteria were removed by centrifugation (Fig. S18, ESI†), most remained in the supernatant. The absorbance and corresponding fluorescence spectra of the supernatants are shown in Fig. 4c. A detailed TEM analysis of these CdS QDs was performed, and the results are presented in Fig. 4d–g. The distribution morphology of these CdS QDs (Fig. 4d, TEM image; Fig. 4e, STEM image) is very different from that of the CdS QDs derived from cadmium acetate (Fig. 3g). These CdS QDs, which are derived from the bioleaching of cadmium ions from

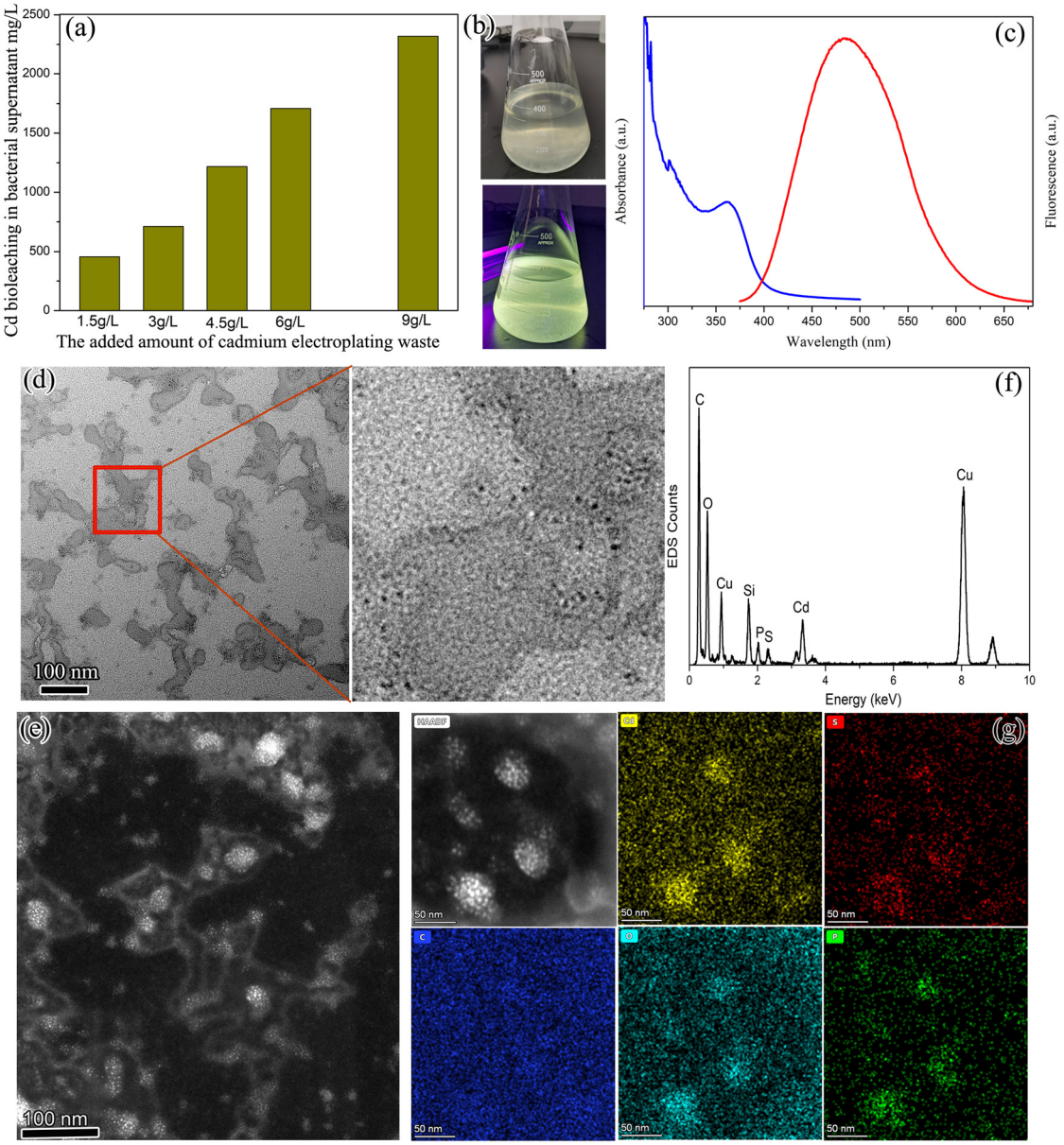

Fig. 4 Waste recycling of cadmium electroplating by *Acidithiobacillus* sp. (a) Relationship between the amount of cadmium electroplating waste added and the bioleaching concentration of cadmium ions in the bacterial supernatant. With the addition of GSH as a cadmium source, CdS QDs can be obtained from the bacterial culture supernatant. (b) Photograph of the *A. caldus* culture supernatant under illumination with white light (above) and UV (365 nm) light (below); obviously, yellow fluorescence in the supernatant can be observed, implying that the CdS QDs were synthesized successfully. (c) Absorbance and corresponding fluorescence spectra of the supernatant at an excitation wavelength of 350 nm. (d) TEM image and (e) combined STEM image showing the size and morphology of the CdS QDs. The elemental information of these CdS QDs is shown in the (f) EDS point scan and (g) EDS maps.

cadmium electroplating waste, are anchored onto dendrimer matrix surfaces, which is similar to the results reported by Liu *et al.*[48] Additionally, the hydrodynamic diameter of these CdS QDs was measured by dynamic light scattering (DynaPro NanoStar, Wyatt Technology), and the results are presented in Fig. S19 in the ESI.† The results revealed four particle sizes as follows: ~2 nm, ~10 nm, ~160 nm, and ~2500 nm. This is basically consistent with our TEM result shown in Fig. 4d. The diameter of single CdS QDs is less than 10 nm, while the formation of a dendrimer matrix leads to a relatively large diameter distributed at ~160 nm and ~2500 nm. The formation of the dendrimer matrix here is likely associated with the significant amount of organic matter present in the initial cadmium electroplating waste (Fig. S16 and S17, ESI†). Fortunately, the CdS QDs generated through this method possess a natural advantage in preventing aggregation. The compositional details of these anchored nanoparticles are illustrated in Fig. 4f and g, confirming that these nanoparticles are indeed CdS QDs.

The CdS QDs derived from cadmium electroplating waste were purified, dried, collected, and subjected to analysis by

X-ray photoelectron spectroscopy (XPS), X-ray diffraction (XRD), and Fourier transform infrared (FTIR) spectroscopy. In addition, the photoluminescence (PL) lifetime of these CdS QDs was also measured. TEM elemental analysis (Fig. 4g) revealed that the chemical composition of the obtained CdS included Cd, S, P, C, and O. This finding was further corroborated by XPS analysis (Fig. 5a), where the high-resolution Cd 3d spectrum (Fig. 5b) exhibited peaks at 404.8 eV and 411.6 eV. The S 2p spectrum (Fig. 5c) confirmed the presence of CdS compounds. The XRD pattern showed broad diffraction peaks corresponding to the (111) and (220) planes of cubic CdS (Fig. 5d), attributed to the small size of the CdS nanoparticles and some amorphous tendencies. The FTIR spectra (Fig. 5e) indicated the presence of surface functional groups on the CdS QDs. Further analysis of these functional groups *via* NMR (^{1}H, ^{13}C, and ^{31}P) (Fig. S20 and S21, ESI†) suggested differences from those of GSH and GSSG, indicating that GSH alone may not be the sole capping agent on the CdS QDs. The time-resolved PL decay profile (Fig. 5f) revealed a fluorescence lifetime of 600.8 ns for the CdS QDs, which was significantly longer than previously reported values.[49] This extended lifetime is attributed to the surface functional groups and dendrimer matrix (Fig. 4d), which effectively prevent nanoparticle aggregation in solutions.[44] The CdS QDs are anchored onto the dendrimer matrix surfaces; therefore, they can maintain good dispersion in aqueous solutions. The hydrodynamic diameter of these CdS QDs was measured by dynamic light scattering (Fig. S19, ESI†), which revealed that most quantum dots (approximately 99.7%) are approximately 2 nm in diameter. Consequently, these favorable factors together promote an improvement in the PL lifetime. The quantum yield (QY) of the CdS QDs is approximately 4.7%, which is similar to that reported for biological CdS QDs produced by other microorganisms or some CdS QDs chemically synthesized in aqueous solutions.[23,50] However, the quantum yield is lower than that of some CdS QDs synthesized by chemical methods.[27,51] Notably, after long-term storage (more than two weeks), a significant decrease in the fluorescence lifetime occurred (Fig. S22, ESI†), indicating unavoidable aggregation and growth of the QDs over time in the solution.

Treating waste Ni–Cd batteries with *Acidithiobacillus* sp. has also been explored, but no ideal CdS QDs have been obtained (Fig. S23, ESI†). Although Cd waste can be effectively bioleached into a solution as Cd^{2+} during the culture of *Acidithiobacillus* sp., during the subsequent process of adjusting the pH of the bacterial solution from acidic to neutral, large quantities of precipitated $Cd(OH)_2$ obviously appear in the solution. In contrast, nearly no $Cd(OH)_2$ precipitation occurred during the pH adjustment of the bacterial bioleaching solution of cadmium electroplating waste. This precipitation phenomenon must be attributed to the lack of large amounts of organic matter contained in the Ni–Cd battery cathode. In the bacterial bioleaching solution of cadmium electroplating waste, large amounts of organic matter (Fig. S16 and S17, ESI†) play an important role in forming complexes with the Cd metal, which not only inhibits $Cd(OH)_2$ precipitation but also promotes the synthesis of the final CdS QDs (Fig. 4).

A schematic of our one-step process for directly realizing the transformation of cadmium waste to CdS QDs by using *Acidithiobacillus* sp. is shown in Fig. 6. Its metabolic products and certain enzymes are fully employed to facilitate this

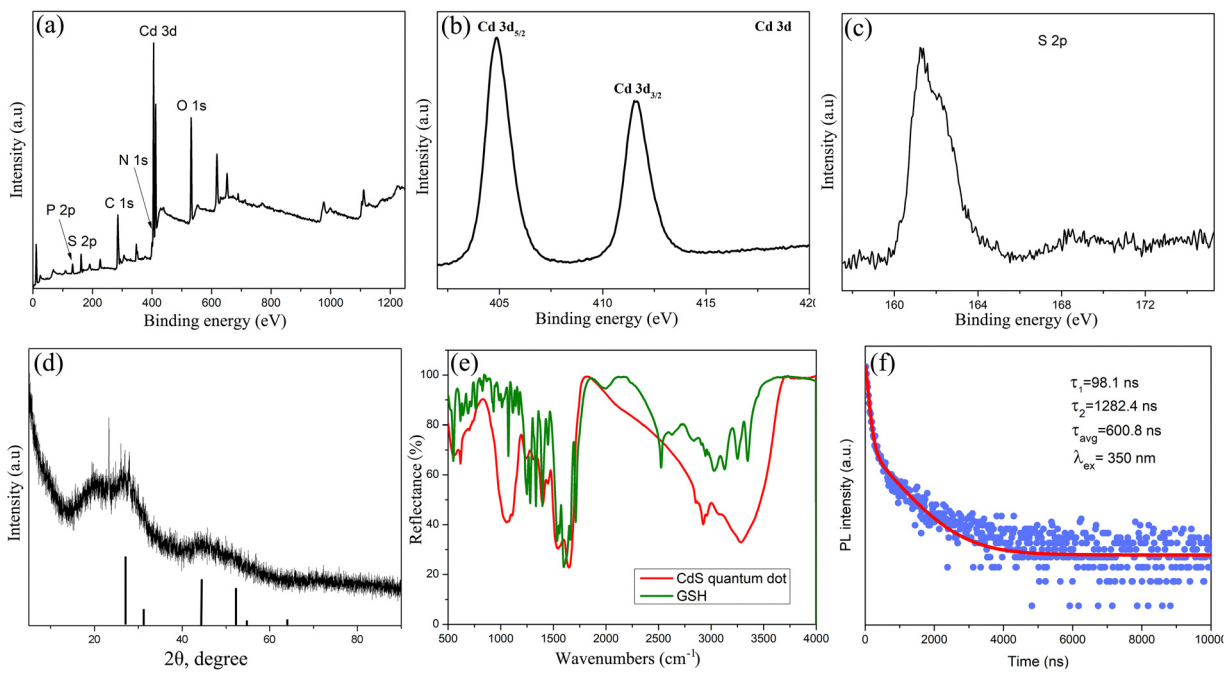

Fig. 5 Further analysis of CdS QDs biosynthesized by *Acidithiobacillus* sp. from cadmium electroplating waste: XPS (a) survey, (b) Cd 3d, and (c) S 2p spectra of the CdS QDs biosynthesized from *Acidithiobacillus* sp. waste. (d) XRD pattern, (e) FTIR spectrum of CdS QDs and GSH, and (f) time-resolved PL decay profile obtained using 375 nm excitation.

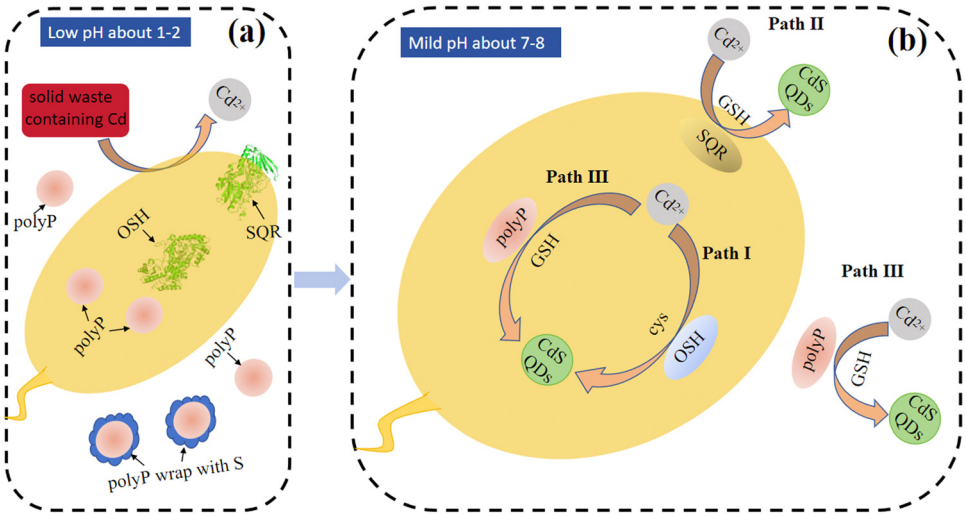

Fig. 6 Schematic of our exploration of one step to directly realize the transformation from cadmium waste to CdS QDs by using *Acidithiobacillus* sp. (a) Cadmium waste can be bioleached into solution during the culture of *Acidithiobacillus* sp. by acids (one of its metabolic products). (b) Cd^{2+} in the culture mixture can be further transformed to CdS QDs *via* the addition of GSH at neutral pH through multiple pathways (*via* the SQR enzyme, OSH enzyme or polyphosphates) in *Acidithiobacillus* sp.

transformation. Three pathways for CdS QDs biosynthesis in *Acidithiobacillus* sp. were revealed: (I) the OSH enzyme pathway, (II) the SQR enzyme pathway and (III) the polyphosphate pathway. Furthermore, the potential of CdS QDs obtained from cadmium electroplating waste by *Acidithiobacillus* sp. as a bioimaging material was evaluated. For this, 4T1 mammary carcinoma cells were cultured in the presence of CdS QDs for 30 min and then examined (Fig. S24, ESI†). Under a confocal laser scanning microscope with excitation at 405 nm, the 4T1 mammary carcinoma cells presented a bright yellow fluorescence signal collected from 510 to 610 nm. In contrast, control cells cultured without CdS QDs appeared nearly dark.

3. Conclusions

Owing to the very unique and complex sulfur metabolic mechanisms in *Acidithiobacillus* sp., there are many enzymes and metabolic products related to sulfur metabolism in this bacterium. The roles of these enzymes and metabolic products in CdS QD biosynthesis were thoroughly revealed in this work. We conducted an exhaustive study and revealed various pathways involved in CdS QD biosynthesis in *Acidithiobacillus* sp. A homologous enzyme of cysteine desulfhydrase exists in *Acidithiobacillus* sp. as an OSH enzyme that is capable of using cysteine as a substrate for the generation of H_2S and then mineralizes CdS from an aqueous cadmium acetate solution. Moreover, structural information for the OSH enzyme was obtained through X-ray crystallography. In addition to the OSH enzyme, two other pathways for CdS QD biosynthesis in *Acidithiobacillus* sp. have been revealed. One pathway involves the SQR enzyme, which catalyzes the conversion of H_2S into sulfur globules and subsequently releases H_2S *via* a reaction with GSH. The liberated H_2S then reacts with cadmium acetate, facilitated by GSH acting as a capping agent, ultimately resulting in the successful synthesis of CdS QDs. The other pathway involves the role of extracellular polyphosphate, which is a metabolic product of *Acidithiobacillus* sp. With the addition of GSH and cadmium acetate, water-soluble fluorescent CdS QDs can be obtained in the supernatant.

Based on our above-described mechanisms of CdS QDs in *Acidithiobacillus* sp., we identified a novel strategy for cadmium waste bioremediation. Finally, we realized the transformation of CdS QDs by *Acidithiobacillus* sp. First, the metabolic products of *Acidithiobacillus* sp., such as inorganic and organic acids, promoted the bioleaching of cadmium metals from cadmium waste into solutions. Furthermore, these bacterial culture solutions with bioleaching cadmium ions were used, and only with the addition of GSH were water-soluble fluorescent CdS QDs successfully obtained from the supernatant. This work provides important insights for cadmium bioremediation, expands the synthesis methods of nanomaterials, advances waste-to-wealth conversion one step forward, and paves the way for cleaner production and a circular economy.

4. Experimental section

4.1. Bacterial strains and growth conditions

The following *Acidithiobacillus* bacterial strains were used in this study: *A. ferrooxidans* ATCC 23270 and *A. caldus* MTH-04. *A. caldus* was cultivated in Starkey-S^0 media (pH 2.5) at 150 rpm and 40 °C. The Starkey culture media used were KH_2PO_4 (3.0 g L^{-1}), $(NH_4)_2SO_4$ (2.0 g L^{-1}), $MgSO_4{\cdot}7H_2O$ (0.5 g L^{-1}), $CaCl_2{\cdot}2H_2O$ (0.25 g L^{-1}), and $FeSO_4{\cdot}7H_2O$ (0.01 g L^{-1}). The solution was dissolved in water, and the pH was adjusted to 2.5 with H_2SO_4. *A. ferrooxidans* was cultivated in 9K-S^0 media (pH 2.5) at 180 rpm and 30 °C. The 9K culture media used were $(NH_4)_2SO_4$ (3 g L^{-1}), K_2HPO_4 (0.5 g L^{-1}), $MgSO_4{\cdot}7H_2O$ (0.5 g L^{-1}), KCl (0.1 g L^{-1}), and $Ca(NO_3)_2$ (0.01 g L^{-1}).

The media were dissolved in water, and the pH was adjusted to 2.5 with H_2SO_4. Before inoculation, 0.8% (w/v) sulfur powder was added to Starkey or 9K liquid media (*i.e.*, 1.2 g of sulfur powder was added to 150 mL of Starkey or 9K liquid media). After 6–7 days, the bacteria were cultivated to the mid-exponential growth phase.

4.2. Expression and purification of the recombinant OSH enzyme

The OSH-encoding gene from either *A. ferrooxidans* or *A. caldus* was cloned and inserted into the pET22b(+) expression plasmid and transferred into *E. coli* BL21 cells for protein expression. Following overnight growth in 10 mL of LB medium supplemented with kanamycin, the cells were inoculated into 1 L of LB broth and cultured at 37 °C with shaking until they reached an OD600 of 0.8. Expression was induced by adding 0.1 mmol L^{-1} IPTG, followed by an overnight incubation at 18 °C. After induction, the bacterial cells were lysed *via* sonication, and the lysate was loaded onto a 5 mL HisTrap high-performance (HP) column (GE Healthcare, USA). The protein was eluted with an imidazole gradient (25 mmol L^{-1} Tris, pH 8.0, 200 mmol L^{-1} NaCl, 20–250 mmol L^{-1} imidazole), followed by passage through a PD-10 column (GE Healthcare, USA) with elution using 25 mmol L^{-1} Tris buffer (pH 8.0, 200 mmol L^{-1} NaCl). The protein was then concentrated using ultrafiltration (MWCO 10 kDa, Millipore) and further purified using a HiloadTM 16/600 SuperdexTM 200 column (GE Healthcare, USA) with elution buffer (25 mmol L^{-1} Tris, pH 8.0, 100 mmol L^{-1} NaCl). SDS-PAGE was used to assess the purity of the collected protein. Finally, the protein was flash-frozen in liquid nitrogen and stored at −80 °C for future use.

4.3. Crystallization of the OSH enzyme

The OSH enzyme was concentrated to 6 mg mL^{-1} by pooling the gel filtration chromatographic peak fractions and then subjected to crystallization trials using the hanging drop vapor diffusion method at 18 °C. Crystals were grown from a solution containing 20% (w/v) polyethylene glycol 3350 and 200 mM magnesium sulfate heptahydrate at pH 5.9 and maintained at 18 °C for 3 days, with further growth continuing for 1 week. Single-crystal X-ray diffraction was conducted using an XtaLAB Synergy DW_Hypix6000 diffractometer. The details of the data collection and structural refinements can be found in the ESI,† Methods.

4.4. CdS QD biosynthesis by the OSH enzyme

OSH (1 mg mL^{-1}) was incubated with 0.5 mM cadmium acetate and 4 mM L-cysteine in 25 mM Tris buffer (pH 8.0, 100 mM NaCl). CdS nanocrystal formation was observed directly in solution over time under UV lamp illumination. The absorbance spectra of the CdS nanocrystals were recorded at regular intervals using a Shimadzu UV-Vis 1800 spectrometer, and the fluorescence emission spectra were measured using a Shimadzu RF-5301PC spectrofluorophotometer with a 350 nm excitation wavelength and a 5-nm excitation slit width.

4.5. Expression and purification of the recombinant SQR enzyme

Recombinant SQR enzyme expression was conducted as described previously.[42] Briefly, the sqr gene was PCR-amplified from *A. caldus* MTH-04 genomic DNA and subsequently cloned and inserted into pTrc99a by the TEDA method, which is a simple and economical approach. A plasmid containing the OSH-encoding gene was constructed and transferred into the *E. coli* MG1655 cell line for protein expression. Bacteria were cultured in 50 mL of LB medium under shaking until they reached an OD600 of 0.5. Subsequently, 0.4 mM IPTG (isopropyl-*b*-D-thiogalactopyranoside) was added, and the cells were further cultured for 4 h before harvesting. The harvested cells were disrupted using an SPCH-18 French press (Stansted Fluid Power Ltd, UK), and the lysate was centrifuged at 20 000 × *g* for 10 min. The supernatant was then ultracentrifuged at 200 000 × *g* for 60 min to isolate the membrane fraction containing the protein, which was subsequently resuspended in Tris–HCl buffer (pH 8.0) with 50 mM DTPA. The protein concentration of the membrane fraction was determined by the BCA method (Beyotime).

4.6. CdS QD biosynthesis by the SQR enzyme

The resuspended membrane fraction containing the SQR enzyme (1 mg mL^{-1}) in Tris–HCl buffer (pH 8.0, with 50 mM DTPA) was used. To this mixture, 1 mM freshly prepared NaHS was added, and the mixture was incubated for 3 h under sealed conditions. Using lead acetate test paper, it was observed that H_2S was completely consumed by the SQR enzyme, resulting in the transformation of H_2S into abundant sulfur globules. Subsequently, 0.5 mM cadmium acetate and 5 mM GSH were added to the solution, which was then placed in a shaker and reacted at 30 °C and 200 rpm. The CdS QD formation was directly monitored over time in solution under UV lamp illumination. The absorbance spectra of the CdS QDs were recorded at regular intervals using a Shimadzu UV-Vis 1800 spectrometer, and the fluorescence emission spectra were recorded using a Shimadzu RF-5301PC spectrofluorophotometer with an excitation wavelength of 350 nm and an excitation slit width of 5 nm.

4.7. Purification of organic fluorescent substances produced by bacteria

After *A. caldus* reached the mid-exponential growth phase, the culture mixture was centrifuged at 10 000 × *g* for 10 min to separate the bacteria. The pH of the resulting supernatant was adjusted to 7.0 using KOH. The mixture was subsequently frozen at −80 °C and subjected to lyophilization using a freeze dryer (Alpha1-4LSC basic). The freeze-dried sample was then dissolved in methanol. This step allows the fluorescent substances produced by the bacteria to dissolve in methanol while removing inorganic salts from the bacterial culture medium. The final sample obtained was analyzed by electrospray ionization mass spectrometry.

4.8. Liquid chromatography-mass spectrometry measurements

The organic fluorescent substances resolved in methanol were analyzed by LC-MS. A C18 column was used to separate substances, and the separated samples were detected by ESI ion chromatography-mass spectrometry (LC-MS) (Ultimate3000 Bruker impact HD, Germany).

4.9. Biosynthesis of CdS QDs by bacterial culture supernatants

After *Acidithiobacillus* sp. reached the mid-exponential growth phase fueled by sulfur, the culture mixture was centrifuged at either 10 000 × *g* for 10 min to remove bacteria or at 2000 × *g* for 10 min to extract the remaining sulfur powder while retaining bacteria. The pH was then adjusted to approximately 7.0 with KOH. Next, 0.5 mM to 1 mM cadmium acetate and 5 mM GSH were added to the solution. If the *Acidithiobacillus* sp. culture had previously been used to bioleach cadmium waste during cultivation, only 5 mM GSH was added. The solution was sealed and incubated for 3 days at 150 rpm and 40 °C. CdS nanoparticle formation in the solution was directly observed under a UV lamp and displayed distinct yellow fluorescence. The absorbance and fluorescence emission spectra of the CdS nanocrystals were recorded, with fluorescence emission spectra measured at an excitation wavelength of 350 nm.

4.10. Purification of CdS QDs

The synthesized CdS QDs distributed in the bacterial culture supernatant were purified as follows. First, the solution was concentrated by rotary evaporation at 37 °C, and then the concentrated solution was applied to a PD-10 column (GE Healthcare, USA) and eluted with deionized water as the buffer.

4.11. Transmission electron microscopy (TEM)

The bacterial cell samples were rinsed with 0.1 M phosphate-buffered saline (pH 7.4) and then suspended in a 1% NaCl solution. A small amount of each cell suspension was applied onto a copper grid coated with a thin layer of amorphous carbon film. Unlike those fixed with glutaraldehyde or dehydrated in ethanol, which dissolves sulfur globules, these cells were not subjected to these treatments. Furthermore, a purified solution containing CdS QDs was placed onto a copper grid coated with a carbon film. All the samples were examined using a Tecnai G2 F20 transmission electron microscope (TEM). Additionally, compositional analysis was performed using a Talos F200X TEM operating at 200 kV, which is equipped with a high-angle annular-dark-field detector and four energy-dispersive X-ray spectrometry (EDS) systems.

4.12. Scanning electron microscopy (SEM)

Samples such as cadmium electroplating waste and Ni–Cd battery cathodes were mounted on carbon conductive adhesive and examined using a Quanta 250 FEG scanning electron microscope (SEM). The SEM instrument was operated at 30 kV and included an energy-dispersive X-ray spectrometry (EDS) system for compositional analysis.

4.13. Nuclear magnetic resonance (NMR) spectroscopy

The CdS QD solution, which was purified and contained 10% D_2O, was prepared for analysis. These samples were transferred into a standard NMR tube (Wilmad) and examined at room temperature using a Bruker AVANCE NEO 600 spectrometer operating at 600 MHz in the ^{1}H, ^{13}C, ^{31}P-frequency mode. Analysis was performed with a 5 mm BBO ultralow-temperature probe head equipped with gradients.

4.14. Time-resolved fluorescence spectroscopy

The purified CdS QD solution was placed into quartz cuvettes with a 1 cm optical path, and time-resolved PL spectra were recorded using an FLS 1000 Edinburgh Instruments spectrofluorimeter. A 980 nm CW diode laser served as the excitation source. The PL decay data were analyzed by fitting them to a triexponential decay model over time (t): $I(t) = A_1 \exp(t/\tau_1) + A_2 \exp(t/\tau_2) + A_3 \exp(t/\tau_3)$, where A_1, A_2, and A_3 denote the amplitudes, and τ_1, τ_2, and τ_3 represent the lifetimes of the three emission components.

4.15. Characterization of the dried powder of purified CdS QDs

After purification, the CdS QDs were dried to obtain a powder. X-ray diffraction (XRD) analysis was performed using a Rigaku Smart Lab 9 kW instrument with Cu Kα (1.542 Å) radiation. The obtained spectra were compared with the standard XRD patterns of CdS (PDF card no. 89-0440) from the International Centre for Diffraction Data (ICDD). X-ray photoelectron spectroscopy (XPS) measurements of the powder samples were also performed using a ThermoFisher ESCALAB 250XI X-ray photoelectron spectrometer. Fourier transform infrared (FTIR) spectroscopy was also conducted using a Bruker VERTEX 70v spectrometer, covering the range of 1000–4000 cm^{-1} with a resolution of 4 cm^{-1}.

4.16. Fluorescence microscopy live imaging of the CdS QDs in cells

For this, 4T1 mammary carcinoma cells were cultured and subsequently incubated for 30 min at 37 °C in the presence of the CdS QD solution. The cells were then observed using a confocal laser scanning microscope (Zeiss LSM 880, Germany) with excitation at 405 nm. Fluorescence signals ranging from 510 to 610 nm were collected during imaging.

Data availability

All relevant data are within the manuscript and its ESI.†

Conflicts of interest

There are no conflicts to declare.

Acknowledgements

This work was supported by the National Natural Science Foundation of China (NSFC) (No. 32271525, 41907105, 32070057, 22102085), and the Instrument Improvement Funds of Shandong University Public Technology Platform (No. ts20220209) and the SKLMT Frontiers and Challenges Project (SKLMTFCP-2023-03). X.-J. Li acknowledges the financial support from Future Program for Young Scholars of Shandong University (No. 62450082164141) and the Instrument Improvement Funds of Shandong University Public Technology Platform (No. ts20220209). T.-Q. Wang acknowledges Shandong province post-doctoral innovation projects of special funds (SDCX-ZG-202303004). We thank N.-N. Dong, J. Zhu, J.-Y. Qu, Z.-F. Li, G.-N. Lin, X.-M. Ren, H.-Y. Sui, S. Wang and Y.-Y. Guo from the core facilities for life and environmental sciences, SKLMT of Shandong University for their assistance in LC–MS/MS, NMR, SEM and laser-scanning confocal microscopy experiments.

References

1 L. Jing, S. V. Kershaw, Y. L. Li, X. A. Huang, Y. Y. Li, A. L. Rogach and M. Y. Gao, *Chem. Rev.*, 2016, **116**, 10623–10730.
2 S. S. Pi, W. J. Yang, W. Feng, R. J. Yang, W. X. Chao, W. B. Cheng, L. Cui, Z. D. Li, Y. L. Lin and N. Q. Ren, *Nat. Sustainability*, 2023, **6**, 1673–1684.
3 K. Sooklal, L. H. Hanus, H. J. Ploehn and C. J. Murphy, *Adv. Mater.*, 1998, **10**, 1083–1087.
4 Z. Kang, Y. Liu and B. Mao, *Quantum dots: Synthesis and Applications*, Science Press, Beijing, China, 2018.
5 C. Murray, D. J. Norris and M. G. Bawendi, *J. Am. Chem. Soc.*, 1993, **115**, 8706–8715.
6 H. Q. Li, X. Wang, J. Q. Xu, Q. Zhang, Y. Bando, D. Golberg, Y. Ma and T. Y. Zhai, *Adv. Mater.*, 2013, **25**, 3017–3037.
7 J. Y. Lee, J. S. Kim, J. C. Park and Y. S. Nam, *Wiley Interdiscip. Rev. Nanomed. Nanobiotechnol.*, 2016, **8**, 178–190.
8 M. Naito, K. Iwahori, A. Miura, M. Yamane and I. Yamashita, *Angew. Chem., Int. Ed.*, 2010, **49**, 7006–7009.
9 A. Aires, M. Moller and A. L. Cortajarena, *Chem. Mater.*, 2020, **32**, 5729–5738.
10 V. Biju, T. Itoh and M. Ishikawa, *Chem. Soc. Rev.*, 2010, **39**, 3031–3056.
11 W. Zhou, Y. Han, B. J. Beliveau and X. H. Gao, *Adv. Mater.*, 2020, **32**, 1908410.
12 Y. Choi and S. Y. Lee, *Nat. Rev. Chem.*, 2020, **4**, 638–656.
13 C. T. Dameron, R. N. Reese, R. K. Mehra, A. R. Kortan, P. J. Carroll, M. L. Steigerwald, L. E. Brus and D. R. Winge, *Nature*, 1989, **338**, 596–597.
14 J. M. Jacob, P. N. L. Lens and R. M. Balakrishnan, *Microb. Biotechnol.*, 2016, **9**, 11–21.
15 G. Gahlawat and A. R. Choudhury, *RSC Adv.*, 2019, **9**, 12944–12967.
16 K. E. Marusak, Y. Feng, C. F. Eben, S. T. Payne, Y. Cao, L. You and S. Zauscher, *RSC Adv.*, 2016, **6**, 76158–76166.
17 C. C. Mi, Y. Y. Wang, J. P. Zhang, H. Q. Huang, L. R. Xu, S. Wang, X. X. Fang, J. Fang, C. B. Mao and S. K. Xu, *J. Biotechnol.*, 2011, **153**, 125–132.
18 S. H. Kang, K. N. Bozhilov, N. V. Myung, A. Mulchandani and W. Chen, *Angew. Chem., Int. Ed.*, 2008, **47**, 5186–5189.
19 K. K. Sakimoto, A. B. Wong and P. D. Yang, *Science*, 2016, **351**, 74–77.
20 Z. Yang, L. Lu, V. F. Berard, Q. He, C. J. Kiely, B. W. Berger and S. McIntosh, *Green Chem.*, 2015, **17**, 3775–3782.
21 N. Bruna, B. Collao, A. Tello, P. Caravantes, N. Díaz-Silva, J. P. Monrás, N. Órdenes-Aenishanslins, M. Flores, R. Espinoza-Gonzalez and D. Bravo, *Sci. Rep.*, 2019, **9**, 1953.
22 L. C. Staicu, P. J. Wojtowicz, M. Pósfai, P. Pekker, A. Gorecki, F. L. Jordan and L. L. Barton, *FEMS Microbiol. Ecol.*, 2020, **96**, fiaa151.
23 V. Carrasco, V. Amarelle, S. Lagos-Moraga, C. P. Quezada, R. Espinoza-González, R. Faccio, E. Fabiano and J. M. Pérez-Donoso, *Microb. Cell Fact.*, 2021, **20**, 41.
24 N. Ma, Z. L. Sha and C. M. Sun, *Environ. Microbiol.*, 2021, **23**, 934–948.
25 X. Huang, Z. Yang, W. Dai, W. Song, Y. Gan, Z. Lian, W. Zhou, Z. Wu, L. Chen and X. Bai, *J. Hazard. Mater.*, 2023, **459**, 132146.
26 M. P. Vena, M. Jobbágy and S. A. Bilmes, *Sci. Total Environ.*, 2016, **565**, 804–810.
27 L. C. Spangler, L. Lu, C. J. Kiely, B. W. Berger and S. McIntosh, *J. Mater. Chem. A*, 2016, **4**, 6107–6115.
28 L. Niu, L. Yu, C. Jin, K. Jin, Z. Liu, T. Zhu, X. Zhu, Y. Zhang and Y. Wu, *Angew. Chem., Int. Ed.*, 2024, **136**, e202315251.
29 R. Dunleavy, L. Lu, C. J. Kiely, S. McIntosh and B. W. Berger, *Proc. Natl. Acad. Sci. U. S. A.*, 2016, **113**, 5275–5280.
30 Y. T. Wang, H. Chen, Z. X. Huang, M. Yang, H. L. Yu, M. C. Peng, Z. Y. Yang and S. D. Chen, *Int. J. Biol. Macromol.*, 2021, **174**, 42–51.
31 J. S. Liu, Z. H. Wang, M. M. Gen and G. Z. Qiu, *Min. Metall. Eng.*, 2006, **26**, 40.
32 R. Wang, J. Q. Lin, X. M. Liu, X. Pang, C. J. Zhang, C. L. Yang, X. Y. Gao, C. M. Lin, Y. Q. Li and Y. Li, *Front. Microbiol.*, 2019, **9**, 3290.
33 L. X. Zhou, *Acta Chim. Sin.*, 2017, **75**, 552.
34 L. Zhao, N. W. Zhu and X. H. Wang, *Chemosphere*, 2008, **70**, 974–981.
35 L. Gan, H. Q. Liu, Q. P. Wang and Z. L. Chen, *China Environ. Sci.*, 2014, **34**, 2617.
36 B. P. Xin, W. F. Jiang, H. Aslam, K. Zhang, C. H. Liu, R. Q. Wang and Y. T. Wang, *Bioresour. Technol.*, 2012, **106**, 147–153.
37 D. Mishra, D. J. Kim, D. E. Ralph, J.-G. Ahn and Y.-H. Rhee, *Waste Manage.*, 2008, **28**, 333–338.
38 Z. W. Zhang, K. Yan, L. Zhang, Q. Wang, R. X. Guo, Z. Y. Yan and J. Q. Chen, *J. Hazard. Mater.*, 2019, **374**, 420–427.
39 P. P. Li and C. S. Peng, *Plat. Surf. Finish.*, 2010, **32**, 37.
40 G. Ulloa, B. Collao, M. Araneda, B. Escobar, S. Álvarez, D. Bravo and J. M. Pérez-Donoso, *Enzyme Microb. Technol.*, 2016, **95**, 217–224.
41 L. F. Li, Z. B. Wang, C. G. Han, H. Q. Sun, R. Wang, Y. L. Ren, J. Q. Lin, X. Pang, X. M. Liu and J. Q. Lin, *J. Appl. Microbiol.*, 2021, **131**, 1800–1812.

42 T. Q. Wang, M. X. Ran, X. J. Li, Y. Q. Liu, Y. F. Xin, H. L. Liu, H. W. Liu, Y. Z. Xia and L. Y. Xun, *Appl. Environ. Microbiol.*, 2022, **88**, e01941.
43 T. Q. Wang, X. J. Li, H. L. Liu, H. W. Liu, Y. Z. Xia and L. Y. Xun, *Sci. Total Environ.*, 2024, **922**, 170504.
44 E. D. Spoerke and J. A. Voigt, *Adv. Funct. Mater.*, 2007, **17**, 2031–2037.
45 J. Huang, K. Sooklal, C. J. Murphy and H. J. Ploehn, *Chem. Mater.*, 1999, **11**, 3595–3601.
46 F. A. Venegas, L. A. Saona, J. P. Monrás, N. Órdenes-Aenishanslins, M. F. Giordana, G. Ulloa, B. Collao, D. Bravo and J. M. Pérez-Donoso, *RSC Adv.*, 2017, **7**, 40270–40278.
47 G. Ulloa, C. P. Quezada, M. Araneda, B. Escobar, E. Fuentes, S. A. Álvarez, M. Castro, N. Bruna, R. Espinoza-González and D. Bravo, *Front. Microbiol.*, 2018, **9**, 234.
48 Z. M. Liu, C. Y. Shao, B. Jin, Z. S. Zhang, Y. Q. Zhao, X. R. Xu and R. K. Tang, *Nature*, 2019, **574**, 394–398.
49 Y. Q. Xu, W. B. Wang, Z. X. Chen, X. Y. Sui, A. C. Wang, C. Liang, J. Q. Chang, Y. H. Ma, L. T. Song and W. Y. Jiang, *Nanoscale*, 2021, **13**, 8004–8011.
50 H. Li, W. Y. Shih and W.-H. Shih, *Ind. Eng. Chem. Res.*, 2007, **46**, 2013–2019.
51 A. Aboulaich, D. Billaud, M. Abyan, L. Balan, J.-J. Gaumet, G. Medjadhi, J. Ghanbaja and R. Schneider, *ACS Appl. Mater. Interfaces*, 2012, **4**, 2561–2569.